UNIVERSITY OF KENTUCKY

May 1, 1985
Technical Report No. JPL 956571-2

For

Contract No. 956571 between the
University of Kentucky Research Foundation and
The California Institute of Technology, Jet Propulsion Laboratory
Stress-Strain Analysis of Silicon Ribbon

by

O. W. Dillon, Jr.
Principal Investigator

This report was prepared for the Jet Propulsion Laboratory, California Institute of Technology, sponsored by the National Aeronautics and Space Administration.

IN PLANE STRESS ANALYSIS

Summary

In light of the discussions concerning the "blowing up" of the UK numerical results for the inplane stress calculations for silicon ribbon, I have decided to prepare this report that ties (I hope) the loose ends together.

The results obtained since January 1985 show that the "blowing up" of computer solutions at least for smooth thermal profiles, is indeed a real physical phenomena. It is our view that they are precisely the "Luder's band" described in the Mobil Solar Quarterly report to JPL for January through March, 1984.

ANALYSIS

The inplane stresses that exist in a thin plate are governed by two general equations (equilibrium and compatability). Equilibrium is used in the form

$$\frac{\partial^2 \sigma_{xx}}{\partial x^2} = \frac{\partial^2 \sigma_{yy}}{\partial y^2} \qquad (1)$$

which contains the normal stresses, σ_{xx} and σ_{yy}. The coordinate system used is shown in Fig. 1. Compatability is assumed in the form

$$\frac{\partial^2 \dot{\varepsilon}_{xx}}{\partial y^2} + \frac{\partial^2 \dot{\varepsilon}_{xy}}{\partial x^2} = \frac{2\partial^2 \dot{\varepsilon}_{xy}}{\partial x \partial y} \qquad (2)$$

which contains the (total) strain rates $\dot{\varepsilon}_{ij}$. Physically compatability is

$$h = N_m b e^{-Q/kT} B(\sqrt{J_2} - D\sqrt{N_m})/\sqrt{J_2}\ \tau_o^m \qquad (5)$$

when $\sqrt{J_2} > D\sqrt{N_m}$, and the parameter J_2 is the second invariant of the deviatoric stress tensor. If $D\sqrt{N_m} > \sqrt{J_2}$ the value of h is zero.

The really novel and extremely important aspect of the Sumino-Haasen model is that the dislocation density changes where shown to vary according to the relationship,

$$\dot{N}_m = K_1\ N_m(\tau - D\sqrt{N_m})^{\lambda+m} e^{-Q/kT} \qquad (6)$$

We now postulate that this same law applies to the situation that occurs in ribbon growth. It will be shown below that having a changing dislocation density is a major effect in modeling real material behavior for the silicon used in solar cell applications.

The major assumption that we are making here is that silicon is assumed to be isotropic in both its elastic and plastic constitutive relations. Eq. (6) happens to fit into the general framework of internal variable theories of viscoplasticity of Dillon and Kratochvil [3]. We sometimes change the parameter K_1 in Eq. (6) to $K_1/10$ in order to approximate a "shape factor" for the ribbon. We now assume that the total strain rate $\dot{\varepsilon}_{ij}$ is the sum of the elastic and plastic parts. Thus our constitutive equation is

$$\dot{\varepsilon}_{ij} = \frac{1+\nu}{E}\dot{\sigma}_{ij} - \frac{\nu}{E}\dot{\sigma}_{KK}\,\delta_{ij} + \alpha\,\dot{T}\,\delta_{ij} + \dot{\varepsilon}_{ij}^{PL} \qquad (7)$$

Steady State

We henceforth assume that the growth process is in a steady state. Thus one can replace derivatives in time by those in the spatial coordinate x. By combining Eqs. (2) and (7), in the steady state we obtain

$$\nabla^2(\sigma_{xx}+\sigma_{yy}) = -\alpha E\nabla^2 T + \frac{1}{v}\int_0^x \left(\frac{\partial^2 \dot{\varepsilon}_{xx}^{PL}}{\partial y^2} + \frac{\partial^2 \dot{\varepsilon}_{yy}^{PL}}{\partial x^2} - 2\frac{\partial^2 \dot{\varepsilon}_{xy}^{PL}}{\partial x \partial y}\right) E\, du \quad (8)$$

where v is the pull speed. In deriving Eq. (8) we neglected spatial derivatives of α and E. In the solution of Eqs. (8), we do allow α and E to vary with temperature and hence with x. In earlier numerical work where $d\alpha/dx$ and dE/dx were retained this assumption was shown to be more than adequate.

When the material is elastic, the solution of Eqs. (1) and (8) is readily accomplished on the digital computer for a specified thermal profile. We have also shown in previous reports that the more analytical procedures given in Boley and Weiner are not adequate for the thermal profiles of interest in the Mobil Solar and Westinghouse processes for growing silicon ribbon. In effect these profiles change too rapidly in space for the Boley-Weiner [4] method to yield good results. On the other hand if $\nabla^2 T$ is constant, the Boley-Weiner method gives excellent agreement with the stresses obtained using finite differences and the digital computer. The ribbon has no external loads applied to it so that stresses are due entirely to the thermal profile.

Dislocation Density

To this writer's knowledge this project is the first ever to use equations such as Eq. (6) for any manufacturing process. That is we explicitly consider the changing internal structure and its effect on stresses and strains that develop during the growth of ribbon.

Most materials researchers normally use materials with large values of the dislocation density. In this case changes in N do not drastically affect the material response. Some solar cell researchers however believe that electronic performance is reduced if the cells have a large number of active dislocations. Silicon people use words such as "dislocation free" silicon for many applications. Certainly it appears that we should consider "low" dislocation densities and one is then forced to consider that they also change when silicon is subjected to stresses. In the growth processes, it is clear that a constitutive model with a changing dislocation density is an important improvement over a model that assumes N_m remains constant.

Westinghouse claims average values of N are 10^2 to $10^3/cm^2$ while Mobil Solar material probably contains 10^5 to $10^6/cm^2$. These numbers apply to the respective final products in both cases.

As will be discussed below, to study how dislocations grow one needs to assume the initial value of N at the melt interface, i.e. the value of N in the solid state at a temperature equal to the solidifying temperature. It turns out that this is a crucial assumption. We decided to try various values for N_0 at the melt interface and to evaluate the validity by comparing the predicted final values of N in the real product. Sometimes this is perfectly satisfactory approach. However we encountered "instabilities" in the numerical scheme and thus could not obtain valid solutions for all of the intended values of N_0 at the melt interface. This raised the question about the validity of our entire numerical code.

Oxygen

While we do not explicitly show how in Eqs. (4) and (6), our computer programs also allow for using different (but uniform) values for the oxygen content. Oxygen content is known to be different for float zone and CZ

IN PLANE STRESS ANALYSIS

Summary

In light of the discussions concerning the "blowing up" of the UK numerical results for the inplane stress calculations for silicon ribbon, I have decided to prepare this report that ties (I hope) the loose ends together.

The results obtained since January 1985 show that the "blowing up" of computer solutions at least for smooth thermal profiles, is indeed a real physical phenomena. It is our view that they are precisely the "Luder's band" described in the Mobil Solar Quarterly report to JPL for January through March, 1984.

ANALYSIS

The inplane stresses that exist in a thin plate are governed by two general equations (equilibrium and compatability). Equilibrium is used in the form

$$\frac{\partial^2 \sigma_{xx}}{\partial x^2} = \frac{\partial^2 \sigma_{yy}}{\partial y^2} \tag{1}$$

which contains the normal stresses, σ_{xx} and σ_{yy}. The coordinate system used is shown in Fig. 1. Compatability is assumed in the form

$$\frac{\partial^2 \dot{\varepsilon}_{xx}}{\partial y^2} + \frac{\partial^2 \dot{\varepsilon}_{xy}}{\partial x^2} = \frac{2\partial^2 \dot{\varepsilon}_{xy}}{\partial x \partial y} \tag{2}$$

which contains the (total) strain rates $\dot{\varepsilon}_{ij}$. Physically compatability is

silicon and to be a major actor in their having differing properties. It is probably different yet for the case of ribbon.

The old EFG thermal profile used is

$$T_4 = 437e^{-1.36x}\cos\pi x + 1157e^{-.066x} - 317e^{-.47}\sin(\frac{\pi x}{2} + \frac{\pi}{6})$$

The modified EFG profile that is used is

$$T_5 = 437e^{-1.36}\cos\pi x + 1157e^{-.066x} - 158.5e^{-.47x}$$

We continue to use

$$T_3 = 1600e^{-.0827x} + 85e^{-5x}\cos\pi x + 75\sin(\pi x/4) - 273$$

as the Westinghouse profile.

RESULTS

We assume thermal profiles which only vary with the distance x from the melt interface. We write Eqs. (1) and (8) in their finite difference approximations and treat the plastic incompatability integral in Eq. (8) as a pseudo thermal field. We then solve Eqs. (1) and (8) by an iterative procedure. The

first iteration is obtained by assuming that the material is elastic, and hence the integral in Eq. (8) is zero. The stresses so obtained are then used in Eqs. (5) and (6) to calculate the plastic strain rates and the dislocation density $N_m(x,y)$ as functions of spatial position. These new plastic strain rates are then used in the integral in Eq. (8), and the whole process repeated. In particular the σ_{yy} stresses at $x = 0$ are determined in the standard way. They are very large and do not relax very much from their elastic values.

Usually 20 iterations suffices for excellent results. Typically values of $\sqrt{J_2}$ are of order 10^8 Pa, while changes in succeeding iterations are usually only 10^2 Pa after 20 iterations.

Typical results for the stresses and the dislocation density are shown in Figs. 2-4. The dislocation density changes by six (or more) orders of magnitude in Fig. (3). As shown in Fig. (2), the stresses eventually decrease in magnitude and N increases so much that of the ribbon is elastic and $\dot{N}_m$ becomes zero.

The data in Fig. (3) show that the value of the melt interface dislocation density that was used is (almost) ridicously small. On the other hand, the final value appears to be representative of ribbon products inferring at least that N_0 is perhaps not too bad.

The plastic strain rates $\dot{\varepsilon}_{xx}^{PL}$ are shown in Fig. 4. Due to the low values of N_0, the plastic strain rates are almost always small compared to the elastic strain rate. Moreover, one finds that the strain rates in the "cusp" region shown in Fig. 4 are <u>very sensitive</u> to the value of N_0 assumed at the melt interface, as can be seen by comparing with the second curve given in Fig. 4. It is relevant that the numerical scheme does not converge for $N_0 = 0.6/cm^2$.

A review of the numerical problem reveals that it is the plastic compatability integral in Eq. (8) which causes the solutions not to converge. This can be understood in view of the "cusp" region in Fig. 4 and noting that compatability requires spatial differentiation of the strain rates. When one considers the basic meaning of compatability, namely that the velocities are required to be single valued functions of space, one decides to look for experimental data for multivalued displacements or velocities.

Such data exists in the Fig. 15 in the Mobil Solar report for January through March of 1984 [5] and has further been seen by us in EFG ribbon. In some cases one can actually see large "jumps" in the deformation field indicating multivalued displacements really do develop. According to personal communication with Dr. J. Kalejs of Mobil Solar, these regions of "Luder's bands" or some other forms of shear banding are developed at 1000°F at stresses of about 25 MPa. Our calculations, show the initial strain rate cusp develops at 1100°F or below and at stresses of 19.7 MPa or above.

EFG Thermal Profile

At this writing, we have obtained convergent solutions for the "old EFG" thermal profile for the case where $N_0 = 1.25 \times 10^{-13}/cm^2$. However we obtain nicely convergent solutions for a modified EFG profile for larger values of N_0. The dislocation density at the melt interface for the modified EFG profile to result in convergent solutions is much below the value of N_0 used in the Westinghouse thermal profile. Numerical solutions for the EFG profile where N_0 is close to the value which results in "unstable" solutions, shows two regions of "cusps" developing in plastic strain rate field in this thermal profile. The cusp near $x = 0$ is very large due to the very large values of σ_{yy} at $x = 0$ in these profiles. Considerably more care is involved in getting stable solutions with an EFG thermal profile as compared to the Westinghouse one.

Said differently, some computer solutions for EFG profile that blow-up are due to the spacing used. However this is not normally the case with the Westinghouse profile. Very very small spacings are needed near x = 0 to avoid blowing up for EFG. The root cause of this problem is the large stresses there.

Inhomogeneous plastic strain rates

Cusps in the plastic strain (rates) such as those shown in Fig. 4 occur also in the case of localized necking of ductile materials. Our localization is (probably) more accurately associated with shear banding than necking. However the analysis below, which parallels that used in necking, is believed to be useful in understanding the complexity of the phenomena shown in Fig. 4. One solves Eq. (3) for the stress and obtains

$$\tau = D\sqrt{N} + \frac{e^{Q/kT}\dot{\varepsilon}^{PL}}{b_o V_o N} \tag{9}$$

The spatial derivative of the stress is

$$\frac{\partial \tau}{\partial x} = \frac{\partial \tau}{\partial N}\frac{\partial N}{\partial x} + \frac{\partial \tau}{\partial T}\frac{\partial T}{\partial x} + \frac{\partial \tau}{\partial \dot{\varepsilon}^{PL}}\frac{\partial \dot{\varepsilon}^{PL}}{\partial x} \tag{10}$$

Since the process is a steady state one, we can write $\partial N/\partial x = \dot{N}/v$ and $\partial\tau/\partial N$, $\partial\tau/\partial T$ and $\partial\tau/\partial\dot{\varepsilon}^{PL}$ can be easily obtained from Eq. (9). Therefore we have

$$\frac{\partial \dot{\varepsilon}^{PL}}{\partial x} = \frac{\frac{\partial \tau}{\partial x} - \frac{\partial \tau}{\partial N}\frac{\dot{N}}{v} - \frac{\partial \tau}{\partial T}\frac{\partial T}{\partial x}}{\frac{\partial \tau}{\partial \dot{\varepsilon}^{PL}}} \tag{11}$$

If one were to consider necking for example, in a constant temperature test in a material where the dislocation density is uniform and constant force, then the R.H.S. of Eq. (11) is zero and the plastic strain rate is uniform in space as well.

In the ribbon growing process however none of the terms on the R.H.S. of the analogue of Eq. (11) vanish and the strain rate in nonuniform is space. As shown in Fig. 4 there are regions where the strain rate is several orders of magnitude larger than it is elsewhere in the ribbon. There is no real simple interpretation of what causes the cusps to develop. Each term in the analogue of Eq. (11) makes a contribution that adds together to cause the "cusps". In the Westinghouse profile with a low melt face dislocation density, $\dot{N}$ is also small near $x = 0$ and the first and last terms on the R.H.S. of Eq. (11) tend to cancel one another. This keeps both $\dot{\varepsilon}^{PL}$ and $\partial\dot{\varepsilon}^{PL}/\partial x$ small. As the dislocation density grows $\dot{N}$ does as well and at $x = 2.5$ cm the cusp has developed as shown in Fig. 4.

The stresses in the (old) EFG profile are very large and nonuniform and this in turn requires very small values of N in order to keep $\dot{\varepsilon}^{PL}$ from getting large and therefore inhomogeneous. Small values of N exist if very small values of N_0 are assumed at the melt interface.

The stresses σ_{yy} at $x = 0$

Hutchinson and Lambropoulos [6] used a finite element method to calculate the stresses in ribbon. They assumed a constitutive equation of the power law type and thereby assume (in effect) that the dislocation density did not change. They also assumed $\sigma_{yy} = 0$ at the melt interface, $x = 0$. Subsequent work by Hutchinson justified this assumption.

Our analysis shows that the σ_{yy} stresses at x = 0, are in fact very large and do not relax very much. An examination of the reason for this reveals that it is because of the low values of N_0 assumed. Both analyses are in fact "correct" and the question is then which is applicable to the growth process. We believe that our analysis is more applicable. We believe that the dislocation density is indeed small and therefore one cannot assume it remains constant.

Adaptive grids

In recent years, it has become good computing practice to let the solution of a problem help distribute the grid points in order to concentrate more points in regions where rapid changes occur. We have incorporated that practice in many of our calculations. Caution is required though lest, the aspect ratio of the grid becomes unsatisfactory. Precautions such as using adaptive grids change the exact values where solutions blow up, but not enough to warrant discussion, at least for a Westinghouse profile.

References

[1] Yonenaga, I. and Sumino, K., Phys. Stat. Sol.(a), Vol. 50, (1978), p. 685. Suezawa, M., Sumino, K. and Yonenaga, I., Phys. Stat. Sol.(a), Vol. 51, (1979), p. 217.

[2] Haasen, P., "Dislocations in the Diamond Structure", Dislocation Dynamics, Edited by Rosenfield, Hahn, Bennett, Joffee, McGraw Hill (1968). Schroter, W., Brion, H. G. and Sietoff, H., J. Appl. Phys., Vol. 54, (1983), p. 1816.

[3] Dillon, O. W. and Kratochvil, J. Appl. Phys., Vol. 40, (1969), p. 3207.

[4] Boley, B. and Weiner, J., Theory of Thermal Stresses, Wiley, New York (1960).

[5] Kalejs, J., Stress Studies in EFG Quarterly Progress Report - Subcontract No. 956312 for January 1, 1984 to March 31, 1984. Mobil Solar Corporation, Walthorn, Mass.

[6] Hutchinson, J. W. and Lambropoulos, J. C., Proceedings of the Flat-Plate Solar Array Project Research Forum on the High-Speed Growth and Characterization of Crystals for Solar Cells, Publication 84-23, Jet Propulsion Laboratory, Pasadena, California.

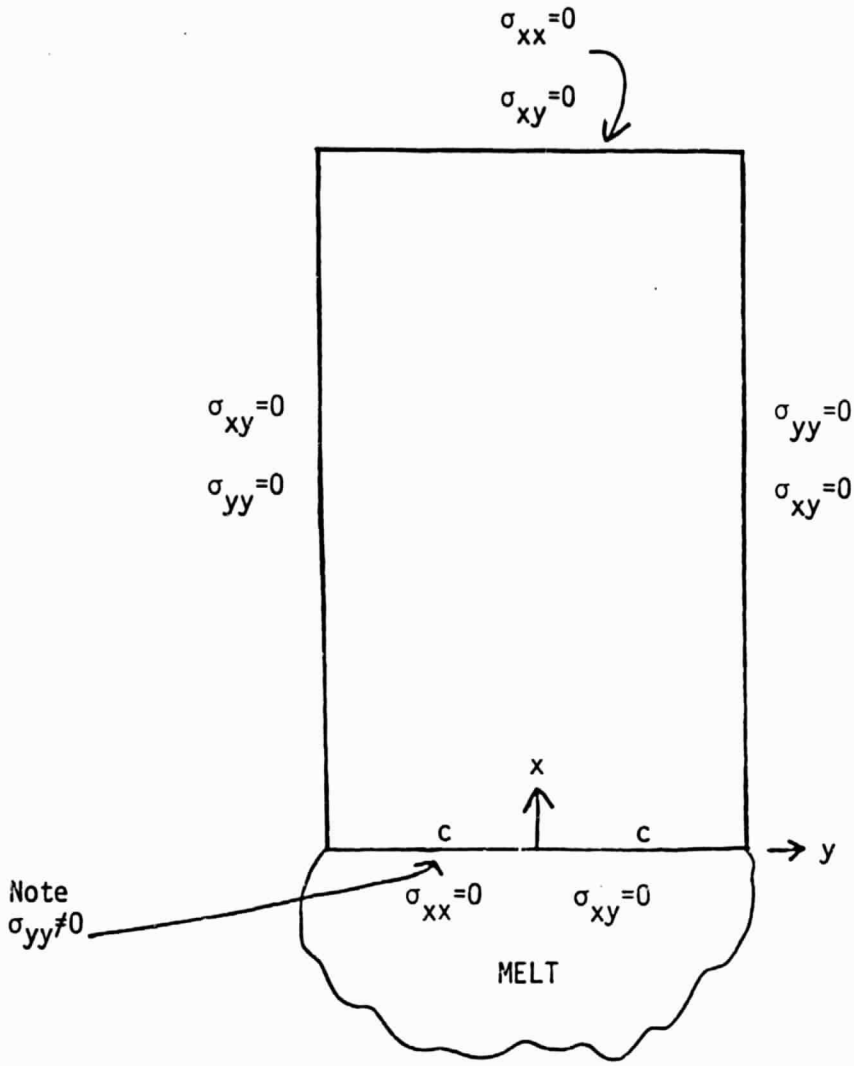

Assumes $t > t_{cr}$

(NO BUCKLING)

Fig. 1

V-0001 17 APR 85

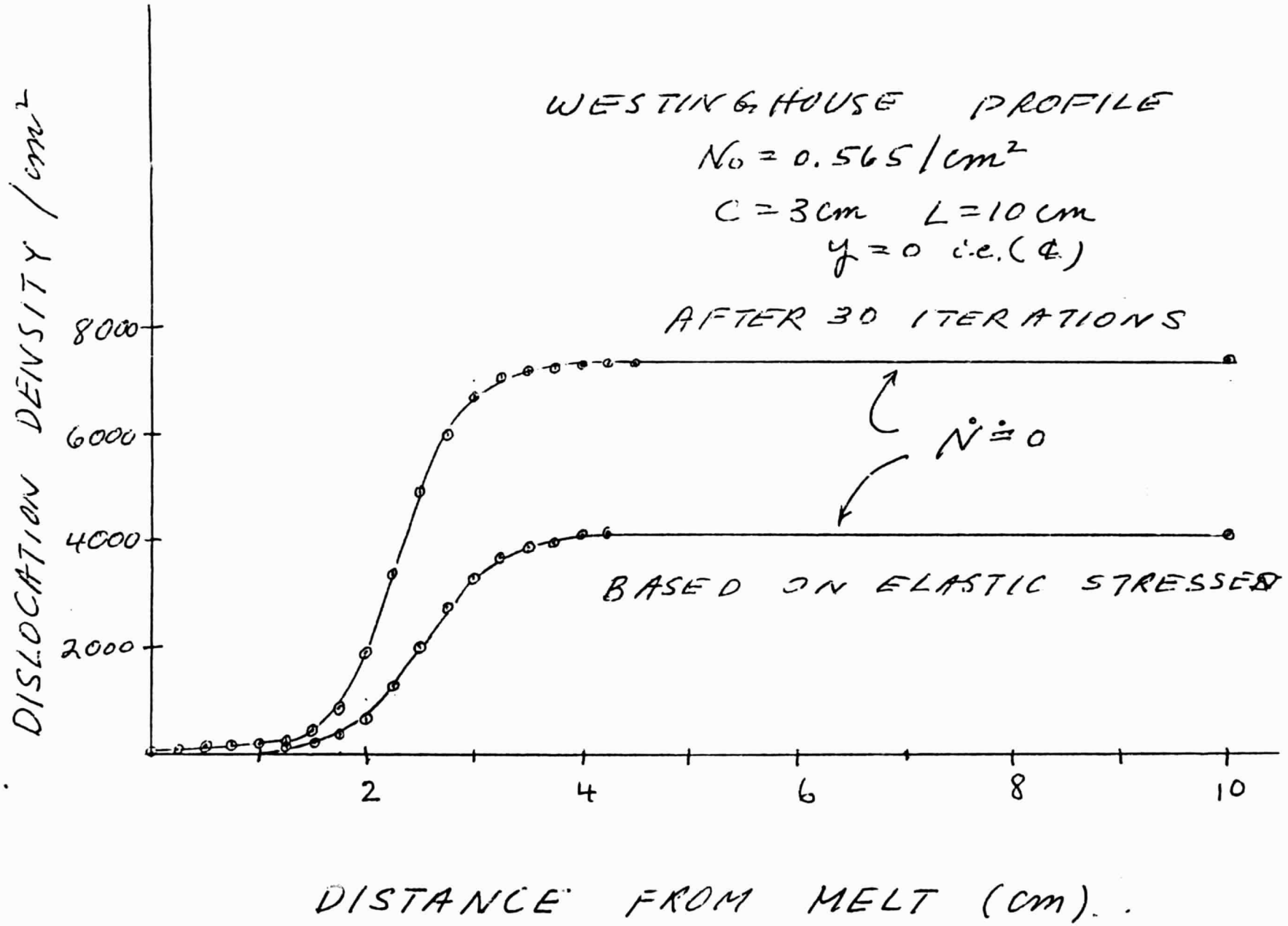

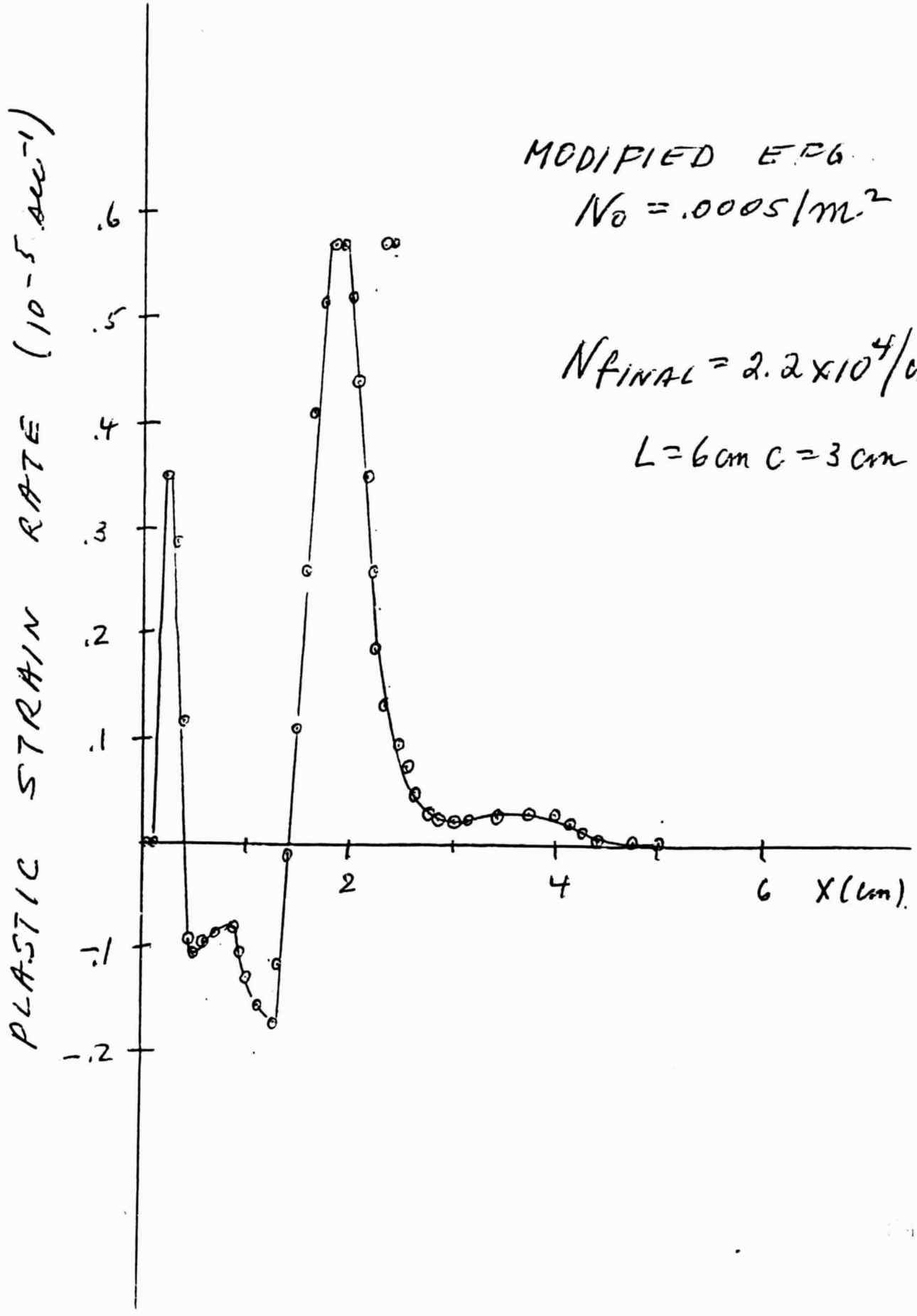
MODIFIED EPG
$N_0 = .0005/m^2$
$N_{FINAL} = 2.2 \times 10^4/cm$
L = 6 cm C = 3 cm
PLASTIC STRAIN RATE (10^{-5} sec^{-1})
.6
.5
.4
.3
.2
.1
-.1
-.2
2
4
6
X (cm)

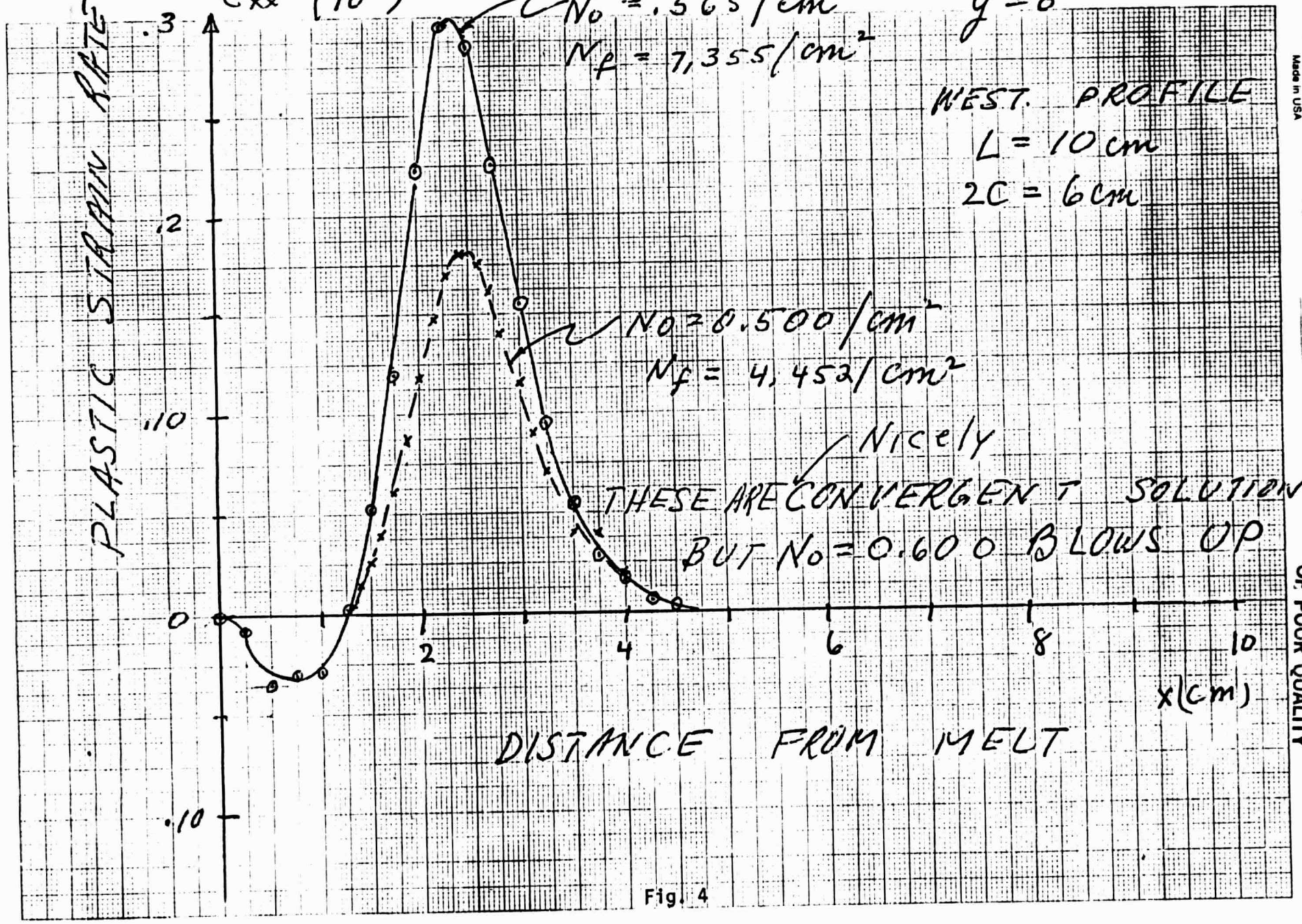

Fig. 4